A Modified Gain Model and the Corresponding Design Method for an *LLC* Resonant Converter

Jianqiang Liu, *Member, IEEE*, Jiepin Zhang, *Student Member, IEEE*, Trillion Q. Zheng, *Senior Member, IEEE*, and Jingxi Yang, *Student Member, IEEE*

***Abstract*—In this paper, a modified gain model and the corresponding design method for an *LLC* resonant converter are proposed. To derive the gain model, two important factors—resonant factor and load factor are considered and discussed in detail by combining time domain and frequency domain. Compared with fundamental harmonic approximation (FHA) method, the accuracy of the gain model is highly improved. Referring to the modified gain model, the corresponding design method is also obtained that can inherit conciseness and practicability of the FHA method. Thus, the design method can be used to replace the FHA method in practical design procedures. Finally, the simulation results are given and a prototype of the *LLC* resonant converter used for power electronic traction transformer is built to verify the accuracy and validity of the proposed gain model and the corresponding design method**

***Index Terms*—Design method, fundamental harmonic approximation (FHA) method, *LLC* resonant converter, modified gain model, power electronic traction transformer (PETT).**

I. Introduction

An *LLC* resonant converter has the features of soft-switching at full range of loads, wide input and output voltage, high efficiency, high power density, electrical isolation, and dual energy flow. So, it is a popular converter and is widely used nowadays [1]–[5]. There are two main application fields of the *LLC* resonant converter, one of which is high frequency switching power supply [6]–[9]. By using the *LLC* resonant converter, the power density will be greatly improved and so do the power quality and conversion efficiency. The typical applications are adapters for electronic equipment, dc/dc converters of photovoltaic system and LED driving, panel TV, and so on. The other one is high voltage and high power field [10]–[14], whose common applications are power electronic transformer, including power electronic traction transformer (PETT) in traction power supply and solid-state transformer in power system, and so on.

When designing an *LLC* resonant converter, if the initial parameters are given, such as rated input and output voltage, current, rated power and working frequency, we usually prefer to discuss the gain characteristic at first and then to conduct further design. Therefore, the precision of the gain model can influence the design results. For precise gain model, the design results can be more accurate that will make benefits for the performance of the *LLC* resonant converter, such as efficiency, control, soft-switching area, and so on. At present, the most common method to derive gain model is fundamental harmonic approximation (FHA) method [15]–[17]. It is an approximation method by calculating fundamental components of the square-wave voltage at primary and secondary side of the *LLC* resonant converter. And then according to the frequency domain analysis, we can easily acquire the gain model whose mathematical expression is concise and practical. However, because the output current is always considered continuously when using FHA method, it will generate much error compared with practical conditions. And with the increasing of load, the error will further increase. To make the gain model derived by FHA method more accurate, some modified methods-based time domain are proposed in [18], [19]. Taking the method in [19], for example, a modified equivalent resistance is calculated by considering the discontinuous current mode. But the analysis of the resonant circuit is not strict and the influence of excitation inductor is neglected, they all make the equivalent resistance and the gain characteristic inaccurate. There are still a few modified gain model based time domains given in [20]–[23]; however, there are too many assumptions being made and the final conclusion is very complicated that make these gain models unpractical. In addition, a new design method considering peak gain is proposed in [24], [25]. The theoretical basis of this method is that when the phase of the input square-wave voltage is the same as the resonant current, the *LLC* resonant converter will get the peak gain point. Based on above theoretical basis, some proper parameters can be calculated and from that the better one can be selected. However, this method has two disadvantages: 1) it is not easy to judge the phase of the input square-wave voltage and the resonant current because of irregularity of the resonant current. 2) All the design results are just satisfied with the peak gain requirement, but the conditions at full frequency range are not discussed. So, the *LLC* resonant converter may operate on the area where the gain increases rapidly and make the dynamic characteristics worse, especially for the high power applications.

In this paper, a modified gain model is proposed. The influence of resonant circuits and load is restudied and the inductor ratio k- and the quality factor Q-based FHA method are redefined. By combining time domain analysis and frequency

Manuscript received June 19, 2016; revised September 4, 2016; accepted October 17, 2016. Date of publication October 31, 2016; date of current version April 24, 2017. This work was supported by the Beijing Science and Technology Plan (2016). Recommended for publication by Associate Editor D. Xu.

J. Liu, J. Zhang, T. Q. Zheng and J. Yang are with the Beijing Jiaotong University, Beijing 100044, China (e-mail: liujianqiang@bjtu.edu.cn; jiepinzhang@bjtu.edu.cn; tqzheng@bjtu.edu.cn; yangjingxi@bjtu.edu.cn).

Color versions of one or more of the figures in this paper are available online at http://ieeexplore.ieee.org.

Digital Object Identifier 10.1109/TPEL.2016.2623418

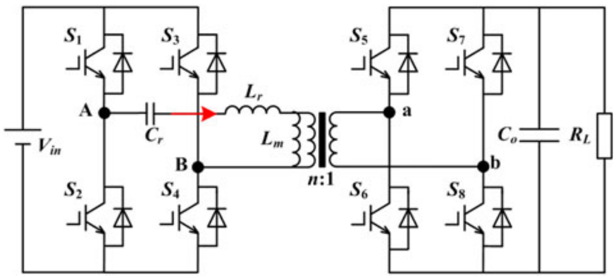

Fig. 1. Topology of the full-bridge *LLC* resonant converter.

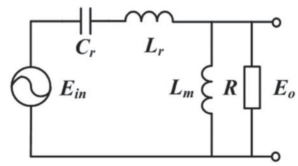

Fig. 2. Equivalent schematic-based FHA method.

domain analysis, the accuracy of the proposed gain model is highly improved at full range of loads making it applicable for both high frequency power supply and high power applications. Based on the proposed modified gain model, a corresponding design method is also given that inherits the conciseness and practicability of the gain models based FHA method. That is, only two degrees of freedom (resonant factor and load factor) are needed to guide the design. According to theoretical analysis, simulations, and experimental results, the feasibility and superiority of the gain model are further verified.

The sections of this paper are organized as follows: Section II simply introduces fundamental principle of FHA method and lists a few definitions for the sake of next analysis. Section III derives the gain model by considering resonant factor and load factor. Section IV proposes a design method based on the proposed modified gain model in Section III. And a design example is given to further describe the design method. Section V verifies the accuracy of the proposed gain model by simulations and experimental results. Section VI concludes this paper.

II. Overview of FHA Method

The topology of a typical *LLC* full-bridge resonant converter is illustrated in Fig. 1. $S_1 - S_4$ and $S_5 - S_8$ are respectively the switches on the primary side and secondary side of the transformer. If dual energy flow is ignored, $S_5 - S_8$ can be replaced by power diodes $D_5 - D_8$. L_r and C_r are resonant inductor and resonant capacitor, respectively, L_m is excitation inductor of transformer, C_o is output filter capacitor, and R_L is load. The ratio of transformer is *n*:1. The direction of the arrow in Fig. 1 is the positive direction mentioned in this paper. Usually, there are three working conditions of the *LLC* resonant converter according to the relationship between switching frequency (f_s) and resonant frequency (f_r) of L_r and C_r. They are continuous mode $(f_s < f_r)$, critical continuous mode $(f_s = f_r)$, and discontinuous mode $(f_s > f_r)$. When FHA method is used, following assumptions and explanations should be done:

1) The *LLC* resonant converter is always working in critical continuous mode, so that the equivalent schematic can be expressed in Fig. 2.
2) The voltage V_{AB} and V_{ab} are continuous square-wave voltages that can be replaced by their fundamental harmonic components. So, they can respectively be expressed as $E_{\text{in}} = \frac{2\sqrt{2}}{\pi} V_{\text{in}}$ and $E_o = \frac{2\sqrt{2}}{\pi} n V_o$ after converting them to the primary side of the transformer.
3) The equivalent ac resistance of the fundamental component is illustrated as $R_{\text{eq}} = n^2 \frac{8}{\pi^2} R_L$.

According to above assumptions and Fig. 2, the gain of the fundamental voltage can be expressed as

$$G_{\text{ac}} = \frac{E_o}{E_{\text{in}}} = \frac{sL_m // R}{\frac{1}{sC_r} + sL_r + sL_m // R}. \quad (1)$$

Let $s = j\omega_s$, where ω_s is switching angular frequency, the gain of the fundamental voltage G_{ac} can be further given as

$$G_{\text{ac}} = \frac{1}{1 + \frac{1}{k}\left(1 - \frac{f_r^2}{f_s^2}\right) + j\left[\frac{f_s}{f_r} - \frac{f_r}{f_s}\right] Q} \quad (2)$$

where $k = \frac{L_m}{L_r}$ and is called inductor ratio. $Q = \frac{\sqrt{L_r/C_r}}{R_{\text{eq}}}$ and is named as quality factor. Then, using $E_{\text{in}} = \frac{2\sqrt{2}}{\pi} V_{\text{in}}$ and $E_o = \frac{2\sqrt{2}}{\pi} n V_o$, the gain of the *LLC* resonant converter can be finally acquired

$$G = \frac{nV_o}{V_{\text{in}}} = \frac{1}{\sqrt{\left[1 + \frac{1}{k}\left(1 - \frac{f_r^2}{f_s^2}\right)\right]^2 + \left[\frac{f_s}{f_r} - \frac{f_r}{f_s}\right]^2 Q^2}}$$
$$= \frac{1}{\sqrt{A^2 + B^2}}. \quad (3)$$

From (3), we can see that the gain characteristic is mainly determined by *k* and *Q*. When resonant inductor L_r and resonant capacitor C_r are constant, *k* and *Q* are respectively influenced by excitation inductance and output resistance. Define $A = 1 + \frac{1}{k}(1 - \frac{f_r^2}{f_s^2})$. It describes the relationship of L_m, L_r, and C_r that is named as resonant factor. Let $B = (\frac{f_s}{f_r} - \frac{f_r}{f_s})Q$. It describes the relationship of R_L, L_r and C_r that is named as load factor.

According to the above introductions, two obvious drawbacks of FHA method are listed:

1) Since the *LLC* resonant converter is always considered working in critical continuous mode, the excitation inductor is always clamped by output voltage. However, in most cases, the *LLC* resonant converter does not work in critical continuous mode and the excitation inductor will have other working conditions which will make resonant factor *A* inaccurate.
2) The equivalent ac resistance is only accurate in critical continuous mode and if $f_s < f_r$, load factor *B* is no more precise.

The two drawbacks make the gain curve derived by FHA method only can describe rough trend but cannot get accurate gain model. Therefore, to acquire optimal gain model,

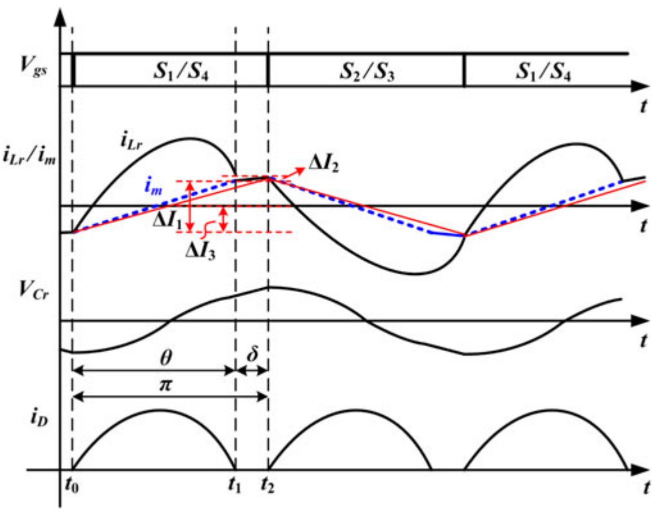

Fig. 3. Theoretical waveform when $f_s < f_r$ ($V_{\rm gs}$ is drive pulses of switches, i_{L_r} is resonant current, i_m is excitation current, V_{C_r} is voltage of resonant capacitor, i_D is current of diode).

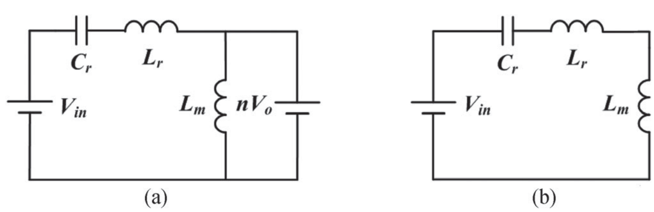

Fig. 4. Equivalent schematics of *LC* resonant mode and *LLC* resonant mode. (a) *LC* resonant mode. (b) *LLC* resonant mode.

we should further modify the resonant factor *A* and load factor *B*.

III. Gain Model Modification

A. Resonant Factor A Modification

To design an *LLC* resonant converter, the most important factor which should be considered is to find the peak gain point. The peak gain point is usually at $f_s < f_r$. Thus, compared with the condition at $f_s > f_r$, the accuracy of the gain curve at $f_s < f_r$ is much more significant. When the *LLC* resonant converter works at $f_s < f_r$, the excitation inductor L_m will not be clamped by output voltage anymore according to Fig. 3. So, it is significant to focus on discontinuous mode. The theoretical waveform when $f_s < f_r$ is given in Fig. 3. For the sake of analysis, several assumptions are proposed: 1) all components are considered ideal, in other words, the influence of dead time, parasitic parameters can be neglected. 2) The output voltage is considered constant which can be equivalent to a voltage source, that is, the influence of load factor *B* can be neglected.

The working condition in halfperiod can be divided into two modes: *LC* resonant mode and *LLC* resonant mode. The two modes respectively correspond to $t_0 - t_1$ and $t_1 - t_2$ in Fig. 3. Their equivalent schematics are shown in Fig. 4.

At t_0, the resonant current $i_{L_r}(t_0)$ is equal to the excitation current $i_m(t_0)$. Let the rising slopes of the excitation current in *LC* resonant mode and *LLC* resonant mode are respectively nV_o/L_r and $nV_o/(L_m + L_r)$. Then, according to the auxiliary lines in Fig. 3, the defined variable ΔI_1, ΔI_2, ΔI_3 can be respectively expressed as

$$\Delta I_1 = \frac{nV_o}{2f_r L_m} \tag{4}$$

$$\Delta I_2 = \frac{V_{\rm in}}{2(L_m + L_r)}\left(\frac{1}{f_s} - \frac{1}{f_r}\right) \tag{5}$$

$$\Delta I_3 = \frac{\Delta I_1 + \Delta I_2}{2} = \frac{1}{2}\cdot\left[\frac{nV_o}{2f_r L_m} + \frac{V_{\rm in}}{2(L_m + L_r)}\left(\frac{1}{f_s} - \frac{1}{f_r}\right)\right] \tag{6}$$

In *LC* resonant mode, the resonant equations can be shown as follows:

$$V_{\rm in} - nV_o = V_{\rm cr}(t - t_0) + L_r\frac{di_{L_r}(t - t_0)}{dt} \tag{7}$$

$$i_{L_r}(t - t_0) = C_r\frac{dV_{\rm cr}(t - t_0)}{dt}. \tag{8}$$

Solve (7) and (8), the voltage of resonant capacitor C_r at time domain can be solved as

$$\begin{aligned} v_{C_r}(t - t_0) = &(V_{\rm in} - nV_o) + (v_{C_r}(t_0) \\ &+ nV_o - V_{\rm in})\cos\omega_r(t - t_0) \\ &+ Z_r i_{\rm Lr}(t_0)\sin\omega_r(t - t_0) \end{aligned} \tag{9}$$

where $\omega_r = 1/\sqrt{L_r C_r}$ and $Z_r = \sqrt{L_r/C_r}$. $v_{C_r}(t_0)$ and $i_{Lr}(t_0)$ are respectively the initial voltage of C_r and the initial current of L_r at t_0. When *LC* mode is finished, that is, after just half-period of resonant period of L_r and C_r, the voltage of C_r can be calculated as

$$v_{C_r}(t_1) = -v_{C_r}(t_0) + 2(V_{\rm in} - nV_o). \tag{10}$$

Then, the *LLC* resonant converter works in *LLC* resonant mode. The duration of *LLC* mode is expressed as

$$\Delta t = \frac{1}{2}\left(\frac{1}{f_s} - \frac{1}{f_r}\right). \tag{11}$$

In this mode, the resonant capacitor is charged by resonant current that is considered being equal to excitation current. The voltage variation can be expressed as

$$\Delta V_1 = \frac{\overline{I_{LLC\ \mathrm{mod}\ e}}}{C_r}\Delta t = \frac{1}{2C_r}\cdot\left(\frac{nV_o}{4f_r L_m} + \frac{nV_o}{4f_s L_m}\right)\Delta t \tag{12}$$

where, $\overline{I_{LLC\ \mathrm{mod}\ e}}$ is average resonant current in *LLC* resonant mode. Considering the nonlinearity of the resonant current in *LLC* resonant mode, $\overline{I_{LLC\ \mathrm{mod}\ e}}$ is usually a bit higher than $\frac{nV_o}{4f_r L_m}$. Thus, the practical $\overline{I_{LLC\ \mathrm{mod}\ e}}$ is approximately selected as $\frac{1}{2}\cdot(\frac{nV_o}{4f_r L_m} + \frac{nV_o}{4f_s L_m})$ as shown in (12). Refer to (10) and (12), the resonant capacitor voltage at t_2 is solved as

$$\begin{aligned} v_{C_r}(t_2) &= v_{C_r}(t_1) + \Delta V_1 \\ &= -v_{C_r}(t_0) + 2(V_{\rm in} - nV_o) + \Delta V_1. \end{aligned} \tag{13}$$

According to the symmetry of resonant capacitor voltage curve, the resonant capacitor voltage at t_0 and t_2 has a

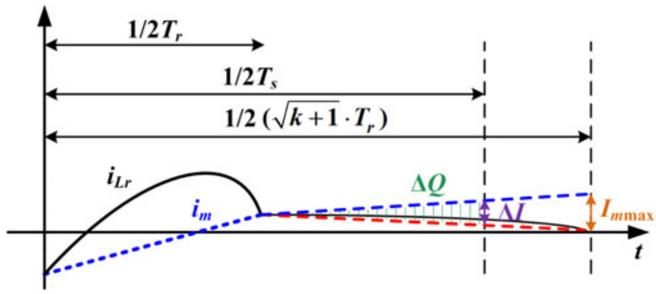

Fig. 5. Theoretical curve of resonant current when switching frequency is far away from resonant frequency.

relationship of

$$v_{C_r}(t_2) = -v_{C_r}(t_0) \tag{14}$$

By summarizing (11)–(14), the following equation can be obtained:

$$2(nV_o - V_{\rm in}) = \frac{nV_o}{16L_m C_r}\cdot\left(\frac{1}{f_s^2}-\frac{1}{f_r^2}\right). \tag{15}$$

Let both sides of (15) divide V_{in}, a gain expression which is not considering the influence of load can be calculated

$$M_1 = \frac{1}{1+\frac{4\pi^2}{32k}\left(1-\frac{f_r^2}{f_s^2}\right)} = \sqrt{\frac{1}{\left[1+\frac{4\pi^2}{32k}\left(1-\frac{f_r^2}{f_s^2}\right)\right]^2}} \tag{16}$$

where M_1 is the gain of the *LLC* resonant converter without considering about the influence of load and $M_1 = nV_o/V_{\rm in}$, $k = L_m/L_r$. The above analysis focuses on the working condition of excitation inductor L_m and mainly modifies the errors of fundamental approximation and continuous assumption. Since the above analysis does not concern about the influence of loads, the results just modify the resonant factor *A*. The modified resonant factor *A* is defined as A_{o1}, which can be expressed as

$$A_{o1} = 1+\frac{4\pi^2}{32k}\left(1-\frac{f_r^2}{f_s^2}\right). \tag{17}$$

The result in (16) and (17) is based on the assumption that the excitation current at the two modes is considered as linear and the rising slopes are respectively nV_o/L_r and $nV_o/(L_m + L_r)$. However, with the decreasing of switching frequency, the gain is close to the peak gain point and the resonant current in *LLC* mode cannot be seemed as linear. And if the value of *k* is small or the switching frequency is close to the peak gain point, the working mode will change from PO mode to PON mode or PN mode, which is discussed in [21] and [24]. For the mentioned situations, the voltage variation of resonant capacitor will be reduced which should be further discussed. Fig. 5 is the theoretical curve of resonant current when switching frequency is far away from resonant frequency of L_r and C_r. For the sake of calculations, the switching period at peak gain point can be approximately regarded as $\sqrt{k+1}\cdot T_r$. According to the resonant current curve shown in Fig. 5, the current variation can be calculated by using similar triangle principle

$$\Delta I = \frac{T_s - T_r}{\left(\sqrt{k+1}-1\right)T_r}\cdot I_{m\,\max}. \tag{18}$$

By summarizing (4)–(6), $I_{m\,\max}$ can be calculated as

$$\begin{aligned} I_{m\,\max} &= \Delta I_1 + \Delta I_2 - \Delta I_3\,\big|_{T_s=\sqrt{k+1}\cdot T_r} \\ &= \frac{nV_o}{4f_r L_m} + \frac{\left(\sqrt{k+1}-1\right)V_{\rm in}}{4\left(L_m+L_r\right)f_r}. \end{aligned} \tag{19}$$

Thus, the current variation can be finally derived as

$$\Delta I = \frac{T_s - T_r}{\left(\sqrt{k+1}-1\right)T_r}\cdot\left[\frac{nV_o}{4f_r L_m} + \frac{\left(\sqrt{k+1}-1\right)V_{\rm in}}{4\left(L_m+L_r\right)f_r}\right]. \tag{20}$$

Then, the shaded area in Fig. 5 that represents the variational quantity of electricity can be given as follows:

$$\Delta Q = \frac{\Delta I\left(T_s - T_r\right)}{4}. \tag{21}$$

By summarizing above equations, the modified voltage variation of the resonant capacitor can be solved as

$$\Delta V'_{C_r} = \Delta V_1 - \frac{\Delta Q}{C_r}. \tag{22}$$

Connect (20), (21) and (22) and let $\Delta V'_{C_r}$ take place of ΔV_1, the gain expression when switching frequency is far away from resonant frequency can be finally calculated as

$$M_2 = \frac{1-\frac{4\pi^2(T_s-T_r)^2 f_r^2}{32(k+1)}}{1+\frac{4\pi^2}{32k}\cdot\frac{(T_s-T_r)^2 f_r^2}{\sqrt{k+1}-1}+\frac{4\pi^2}{32k}\left(1-\frac{f_r^2}{f_s^2}\right)} \tag{23}$$

where M_2 is the gain of the *LLC* resonant converter without considering about the influence of load when PON mode or PN mode is discussed. That is, the modified resonant factor *A* when switching frequency is far away from resonant frequency can be expressed as

$$A_{o2} = \frac{1+\frac{4\pi^2}{32k}\cdot\frac{(T_s-T_r)^2 f_r^2}{\sqrt{k+1}-1}+\frac{4\pi^2}{32k}\left(1-\frac{f_r}{f_s}\right)}{1-\frac{4\pi^2(T_s-T_r)^2 f_r^2}{32(k+1)}}. \tag{24}$$

Here, A_{o1} and A_{o2} are all significant. In practical design process, A_{o1} and A_{o2} should be reasonably chosen according to their respective working conditions. If the working area is not close to the peak gain point, A_{o1} is much preferred. And inversely, if switching frequency is far away from resonant frequency, A_{o2} is highly desired.

B. Load Factor B Modification

The *LLC* resonant converter is usually considered working in continuous mode all the time when FHA method is used to discuss the influence of load. That is, no matter how frequency changes, the equivalent ac resistance is always the same as the value in critical continuous mode which is $n^2\frac{8}{\pi^2}R_L$. However, in many cases the *LLC* resonant converter usually works in discontinuous mode rather than critical continuous mode. Thus, the practical equivalent ac resistance will change along with the switching frequency rather than a constant value. Meanwhile, it is known that with the increasing of load, the influence of load factor *B* is enhanced so the error of FHA method will further increase. The practical gain curve and the gain curve derived by

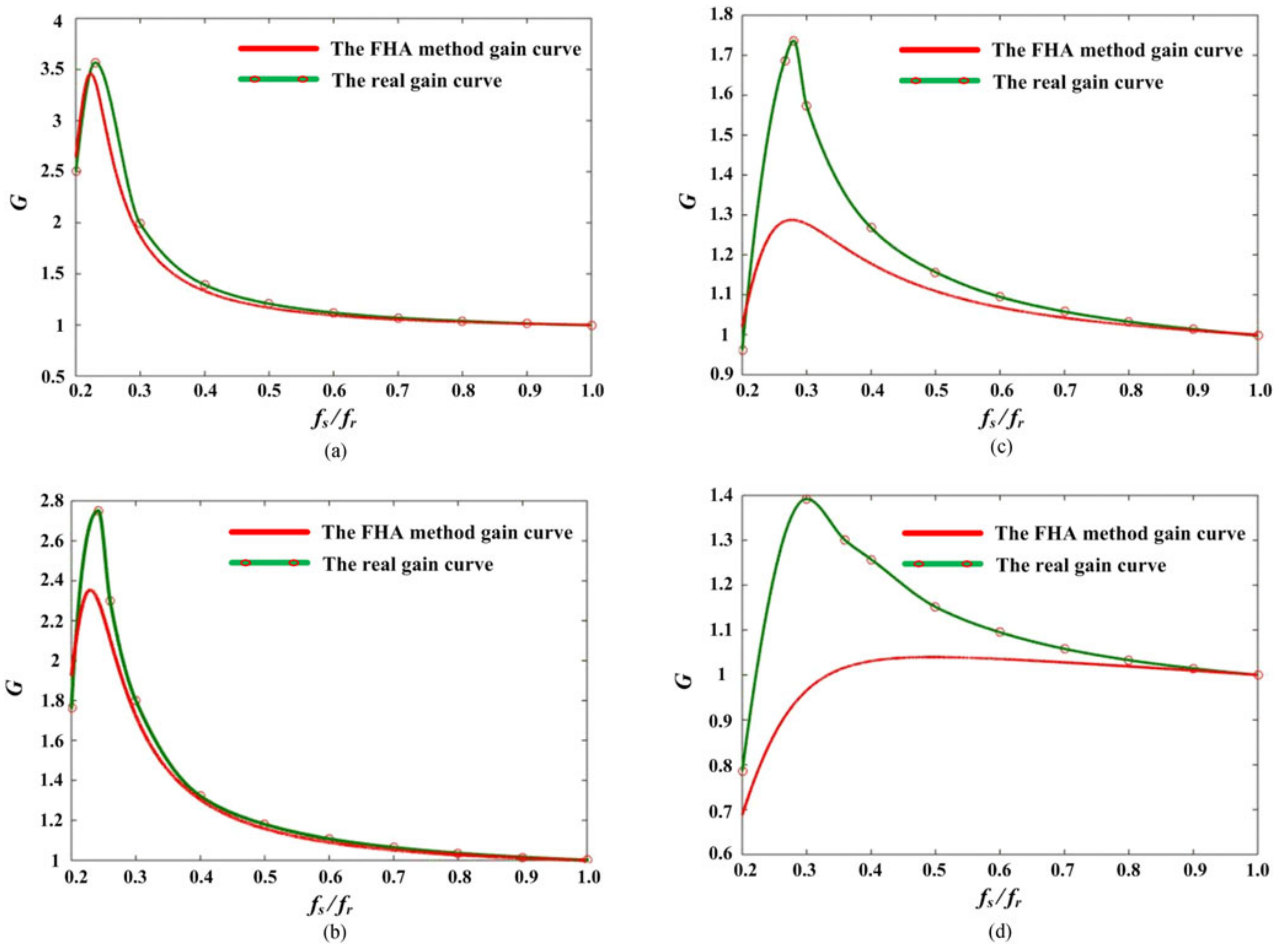

Fig. 6. Real gain curve and the gain curve derived by FHA method when $k = 20$. (a) $Q = 0.05$. (b) $Q = 0.1$. (c) $Q = 0.2$. (d) $Q = 0.3$.

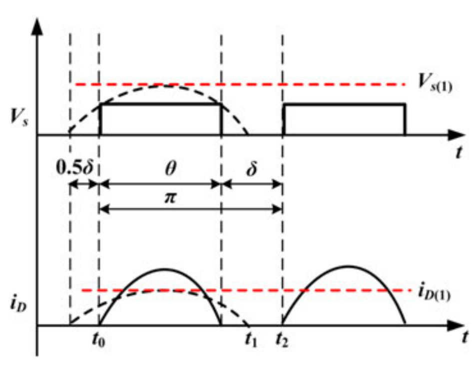

Fig. 7. Theoretical voltage and current curves in secondary side rectifier of *LLC* resonant converter in discontinuous mode.

FHA method with different quality factor Q are represented in Fig. 6. According to the comparisons in Fig. 6, it can be seen that with the increasing of load, the error caused by the FHA method becomes pretty large. When the quality factor $Q > 0.2$, the gain curves have been totally distorted.

To acquire more precise gain model, this paper discusses and calculates the value and phase of the equivalent ac resistance. Fig. 7 indicates the theoretical voltage and current curves at secondary side of the *LLC* resonant converter in discontinuous mode, where V_s is the voltage of transformer in secondary side when active power is transferred to load ($V_s = 0$ means the *LLC* resonant converter does not transfer active power to load). i_D is the current of the diodes.

In the course of the study, assume the current of the diode is a sinusoidal pulse. In half-period, the turn-on angle is θ, and the extinction angle is δ. It is obvious that $\theta+\delta = \pi$, and the current of the diodes can be expressed as

$$i_D = \begin{cases} I_D \sin(\omega_r t) & [t_0 - t_1] \\ 0 & [t_1 - t_2] \end{cases}. \tag{25}$$

Here, I_D is the peak value of diode current. According to charge conservation principle, the relationship of I_D and average output current I_o can be given as

$$\int_{t_0}^{t_1} I_D \sin(\omega_r t)\, dt = I_o \cdot (t_2 - t_0). \tag{26}$$

Solve (26) and use the defined angle θ in Fig. 7, I_D can be calculated as

$$I_D = I_o \frac{\pi^2}{2\theta}. \tag{27}$$

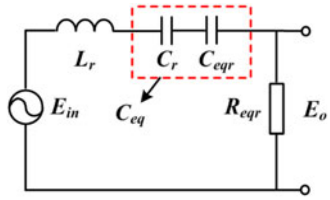

Fig. 8. Equivalent schematic in discontinuous mode.

By Fourier transformation, the fundamental components of V_s and i_D that are shown in Fig. 7 can be represented by

$$V_{s(1)} = V_o \frac{4}{\pi} \sin \frac{\theta}{2} \tag{28}$$

$$I_{D(1)} = I_D \frac{\theta - \sin\theta}{\pi} = I_o \frac{\pi(\theta - \sin\theta)}{2\theta}. \tag{29}$$

Then, the modified equivalent ac resistance $R_{\rm eqr}$ that is converted to the primary side of transformer is sloved as

$$R_{\rm eqr} = n^2 \frac{V_{s(1)}}{I_{D(1)}} = n^2 \frac{8}{\pi^2} \frac{\theta \sin\frac{\theta}{2}}{\theta - \sin\theta} R_L. \tag{30}$$

From Fig. 7, the differences of the equivalent ac resistance between the proposed method and FHA method are not only shown in values but also shown in phases. And, the phase difference is 0.5δ according to Fig. 7. Thus, the modified equivalent load is not just resistive load but is the mix of capacitive load and resitive load. Let the value of the modified load is $X_{\rm eqr}$, and $X_{\rm eqr} = R_{\rm eqr} + \frac{1}{j\omega_s C_{\rm eqr}}$, where $C_{\rm eqr}$ is the equivalent capacitance. Since the phase difference is 0.5δ, $C_{\rm eqr}$ can be represented by

$$C_{\rm eqr} = \frac{1}{\omega_s R_{\rm eqr} \tan\left(\frac{\delta}{2}\right)}. \tag{31}$$

According to above results, the equivalent schematic in discontinuous mode can be expressed in Fig. 8.

The series of C_r and $C_{\rm eqr}$ can be further combined as $C_{\rm eq}$

$$C_{\rm eq} = \frac{C_r}{\omega_s R_{\rm eqr} \tan\left(\frac{\delta}{2}\right) \cdot \left(C_r + \frac{1}{\omega_s R_{\rm eqr} \tan\left(\frac{\delta}{2}\right)}\right)}. \tag{32}$$

Refer to the expression $Q = \frac{\sqrt{L_r/C_r}}{R_{\rm eq}}$ derived by FHA method, the modified quality factor Q_o can be shown in the following equation:

$$Q_o = \frac{\sqrt{\frac{L_r \omega_s R_{\rm eqr} \tan\left(\frac{\delta}{2}\right) \cdot \left(C_r + \frac{1}{\omega_s R_{\rm eqr} \tan\left(\frac{\delta}{2}\right)}\right)}{C_r}}}{R_{\rm eqr}}. \tag{33}$$

By summarizing (30) and (33), the modified load factor B_o can be solved as equation (34) as shown bottom of this page.

In this part, for the sake of analysis and calculations, the angle is used to replace frequency. The relationships of the angles and frequency are complementary as $\theta = \frac{f_s}{f_r}\pi$, $\delta = (1 - \frac{f_s}{f_r})\pi$.

C. Gain Model Modification

Part A and Part B respectively modify the resonant factor *A* and load factor *B* that are introduced in Section II. And, finally the modified resonant factor A_o and load factor B_o are calculated. Substitute them into (3) to replace *A* and *B*, the modified gain model of the *LLC* resonant converter can be acquired. If the resonant factor *A* is replaced by A_{o1} in (17), the gain can be expressed as (35). And, G_{o1} is applicable for the condition whose working area is $0.75\sqrt{k+1}T_r - T_r$. Analogously, if the resonant factor *A* is replaced by A_{o2} in (22), the gain can be expressed as (36). And, G_{o2} is applicable for the condition whose switching period area is $\sqrt{k+1}T_r - 0.75\sqrt{k+1}T_r$. equation (35) as shown on the bottom of this page and equation (36) as shown on the bottom of the next page.

$$B_o = \left(\frac{f_s}{f_r} - \frac{f_r}{f_s}\right) \frac{\sqrt{\frac{L_r \omega_s n^2 \frac{8}{\pi^2} \frac{\theta \sin\frac{\theta}{2}}{\theta - \sin\theta} R_L \tan\left(\frac{\delta}{2}\right) \cdot \left(C_r + \frac{1}{\omega_s n^2 \frac{8}{\pi^2} \frac{\theta \sin\frac{\theta}{2}}{\theta - \sin\theta} R_L \tan\left(\frac{\delta}{2}\right)}\right)}{C_r}}}{n^2 \frac{8}{\pi^2} \frac{\theta \sin\frac{\theta}{2}}{\theta - \sin\theta} R_L}. \tag{34}$$

$$\begin{aligned} G_{o1} &= \frac{1}{\sqrt{\left[1 + \frac{4\pi^2}{32k}\left(1 - \frac{f_r}{f_s}\right)\right]^2 + \left[\frac{f_s}{f_r} - \frac{f_r}{f_s}\right]^2 \frac{L_r \omega_s n^2 \frac{8}{\pi^2} \frac{\theta \sin\frac{\theta}{2}}{\theta - \sin\theta} R_L \tan\left(\frac{\delta}{2}\right) \cdot \left(C_r + \frac{1}{\omega_s n^2 \frac{8}{\pi^2} \frac{\theta \sin\frac{\theta}{2}}{\theta - \sin\theta} R_L \tan\left(\frac{\delta}{2}\right)}\right)}{C_r \left(n^2 \frac{8}{\pi^2} \frac{\theta \sin\frac{\theta}{2}}{\theta - \sin\theta} R_L\right)^2}}} \\ &= \frac{1}{\sqrt{\left[1 + \frac{4\pi^2}{32k}\left(1 - \frac{f_r}{f_s}\right)\right]^2 + \left[\frac{f_s}{f_r} - \frac{f_r}{f_s}\right]^2 Q_o^2}} \end{aligned} \tag{35}$$

IV. Design Procedure

It is known that the gain model derived by the FHA method contains notable error. The error will become much more evident with the increasing of load. If the gain expression that is shown in (3) is used to design parameters of the *LLC* resonant converter, it is pretty hard to get satisfied results to achieve good characteristics. Taking Fig. 6(d) as an example, the peak gain derived by the FHA method is only 1.03. However, the real peak gain is approximately 1.4. That is, if we use the FHA method to lead the design, only smaller Q can feed the requirement. When other conditions are not changed, reducing Q will decrease resonant inductance L_r. Since $k = L_m/L_r$, the excitation inductance will reduce, too. And, according to (19), the maximum excitation current will increase which will lead higher turn-off switching loss to reduce efficiency.

Though the FHA method has above mentioned disadvantages, it is still widely used in the design of the *LLC* resonant converter because of its simplicity. During the design process, only two degrees (inductor ratio k and quality factor Q) should be considered. And once k and Q are calculated, the parameters of the *LLC* resonant converter can be directly solved. This paper focuses on the disadvantages of the FHA method and modify the gain model by time domain analysis and frequency domain analysis. For the modified gain model, on the one hand, it improves the precision of conventional gain model and on the other hand, the design idea of FHA method is still retained that makes the design more simple.

The design procedure of the modified gain model is proposed as follows and the recommended software design flow diagram is given in Fig. 9.

1) Calculate transformer ratio n and maximum gain value $G_{\max}$ according to the design requirements. Usually, the design requirements of the *LLC* resonant converter mainly include input voltage range $(V_{\text{in min}} - V_{\text{in max}})$, rated output voltage (V_o), rated power (P_o), and resonant frequency (f_r). Since the *LLC* resonant converter is a kind of boost converter when $f_s < f_r$, the transformer ratio should be calculated by using the maximum input voltage that is expressed as

$$n \geq \frac{V_{\text{in max}}}{V_o}. \tag{37}$$

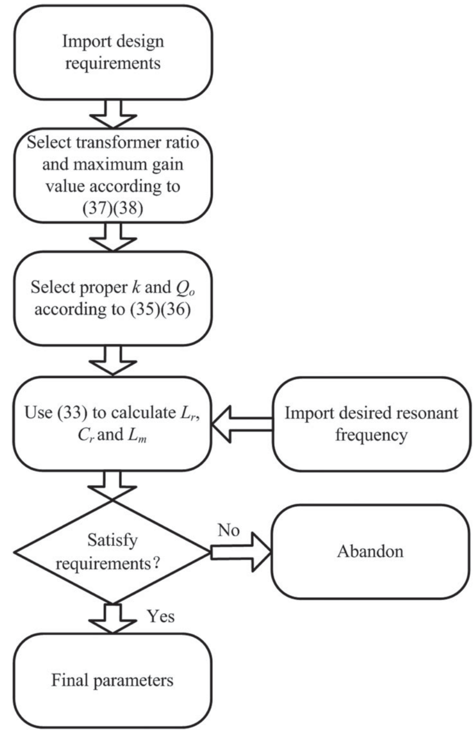

Fig. 9. Recommended software design flow diagram.

Then, the peak gain requirement $G_{\max}$ can be calculated as

$$G_{\max} \geq \frac{nV_o}{V_{in\,\min}}. \tag{38}$$

2) Substitute different k and Q_o into (35) or (36) to draw the corresponding gain curve. If the working area is not close to the peak gain point, (35) is preferred, otherwise, (36) should be used. The precise calculation results are given in [24] which can help determine whether (35) or (36) should be used. In practical use, it is not necessary to calculate such precise value. According to (18) and combined with simulation and experimental results, the recommended switching period area using A_{o2} is $\sqrt{k+1}T_r - 0.75\sqrt{k+1}T_r$ and the recommended switching period area using A_{o1} is $0.75\sqrt{k+1}T_r - T_r$.Then, select proper k and Q_o which can exactly satisfy the requirement of the $G_{\max}$

$$G_{o2} = \frac{1}{\sqrt{\left[\frac{1+\frac{4\pi^2}{32k}\cdot\frac{(T_s-T_r)^2 f_r^2}{\sqrt{k+1}-1}+\frac{4\pi^2}{32k}\left(1-\frac{f_r}{f_s}\right)}{1-\frac{4\pi^2 (T_s-T_r)^2 f_r^2}{32(k+1)}}\right]^2 + \left[\frac{f_s}{f_r}-\frac{f_r}{f_s}\right]^2 \frac{L_r\omega_s n^2 \frac{8}{\pi^2}\frac{\theta\sin\frac{\theta}{2}}{\theta-\sin\theta}R_L\tan\left(\frac{\delta}{2}\right)\cdot\left(C_r+\frac{1}{\omega_s n^2\frac{8}{\pi^2}\frac{\theta\sin\frac{\theta}{2}}{\theta-\sin\theta}R_L\tan\left(\frac{\delta}{2}\right)}\right)}{C_r\left(n^2\frac{8}{\pi^2}\frac{\theta\sin\frac{\theta}{2}}{\theta-\sin\theta}R_L\right)^2}}}$$

$$= \frac{1}{\sqrt{\left[\frac{1+\frac{4\pi^2}{32k}\cdot\frac{(T_s-T_r)^2 f_r^2}{\sqrt{k+1}-1}+\frac{4\pi^2}{32k}\left(1-\frac{f_r}{f_s}\right)}{1-\frac{4\pi^2 (T_s-T_r)^2 f_r^2}{32(k+1)}}\right]^2 + \left[\frac{f_s}{f_r}-\frac{f_r}{f_s}\right]^2 Q_o^2}}. \tag{36}$$

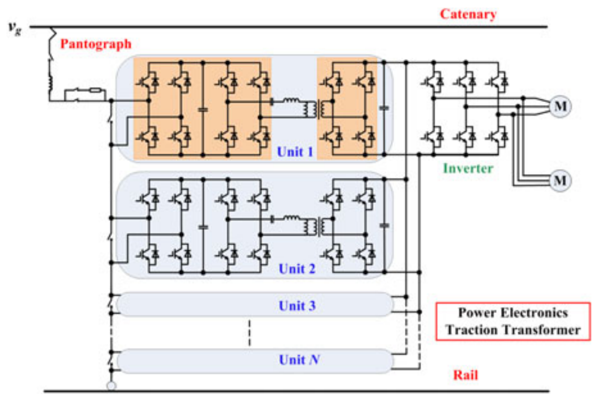

Fig. 10. Structure of PETT.

TABLE I
DESIGN REQUIREMENTS OF *LLC* CONVERTER

Parameters	Values
Input voltage	350($\pm$ 10) V
Output voltage	120 V
Switching frequency	3–5 kHz
Maximum power	3 kW

3) Use Q_o to calculate the relationship between resonant inductance L_r and resonant capacitance C_r according to (33). It is necessary to point that the expression of Q_o is a variable of switching frequency, so we should select desired switching frequency point at first.
4) Use the results calculated in step 3 and combine $f_r \geq 1/2\pi\sqrt{L_r C_r}$ to obtain resonant inductance L_r and resonant capacitance C_r. Then, use $k = L_m/L_r$ to calculate excitation inductance L_m.
5) Substitute the calculated parameters into (35) or (36) and verify the validity of the design results.

To support the design procedure, a design example of PETT is represented. The structure of PETT is shown in Fig. 10 whose dc–dc link is composed of the *LLC* resonant converter. The design requirements of one unit of the *LLC* resonant converter are shown in Table I. First, the input voltage range is 340—360 V and the output voltage is 120 V. By considering (35), the transformer ratio can be calculated as $n \geq 3$. To be corresponding to the transformer ratio of the experimental prototype, let $n = 3.144$. Then, the peak gain requirement $G_{\max} = 1.11$ can be acquired by using (36). From Table I, the frequency range is 3–5kHz, which means that the gain should be high than 1.11 when $f_s = 3$ kHz.

After determining the values of transformer ratio and peak gain requirement, k and Q_o should be discussed. As for k, in medium and high power applications such as PETT, it is usually a bit large. There are two main reasons: 1) the high frequency transformer with small k will be produced hardly when the power level is very high. 2) Large k can improve the control characteristic in the effective working range. In this paper, k is selected as 20 referring to [12] and which is corresponding to the experimental prototype. Then, substitute $k = 20$ respectively into

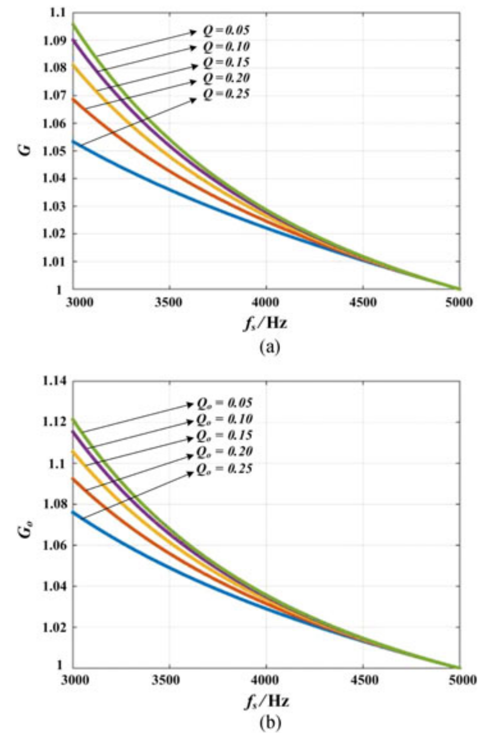

Fig. 11. Gain curves with different Q or Q_o based FHA method and the proposed modified gain model. (a) FHA method. (b) Modified gain model.

TABLE II
PARAMETERS OF THE *LLC* RESONANT CONVERTER

Parameters	Values
Input voltage $V_{\rm in}$	350($\pm$ 10) V
Output voltage V_o	120 V
Transformer ratio *n:1*	3.144:1
Resonant inductance L_r	111 μH
Resonant capacitance C_r	9 μF
Excitation inductance L_m	2.22 mH

(3) and (35), the comparisons of the gain curves with different Q or Q_o are obtained from the FHA method, and the proposed gain model is given in Fig. 11. For the proposed gain model, it is obvious that when $Q_o < 0.15$, the peak gain requirement can be satisfied. However, for the gain curves based FHA method, even no available Q can be selected to feed the peak gain requirement which further verify the inaccuracy of the FHA method.

According to Fig. 11, the gains of $Q_o = 0.15$ and $Q_o = 0.10$ at 3 kHz are respectively 1.105 and 1.115. To satisfy the requirement of the peak gain, which is $G_{\max} = 1.11$, Q_o should be satisfied with $0.1 < Q_o < 0.15$. Thus, choose $Q_o = 0.13$ as the final modified quality factor. And, the turn-on angle θ and rated resistance can be calculated as follows:

$$\theta = \frac{f_s}{f_r}\pi = 0.6\pi \tag{39}$$

$$R_L = \frac{V_o^2}{P_{o\max}} = 4.8\,\Omega \tag{40}$$

$$f_r = \frac{1}{2\pi\sqrt{L_r C_r}} = 5000. \tag{41}$$

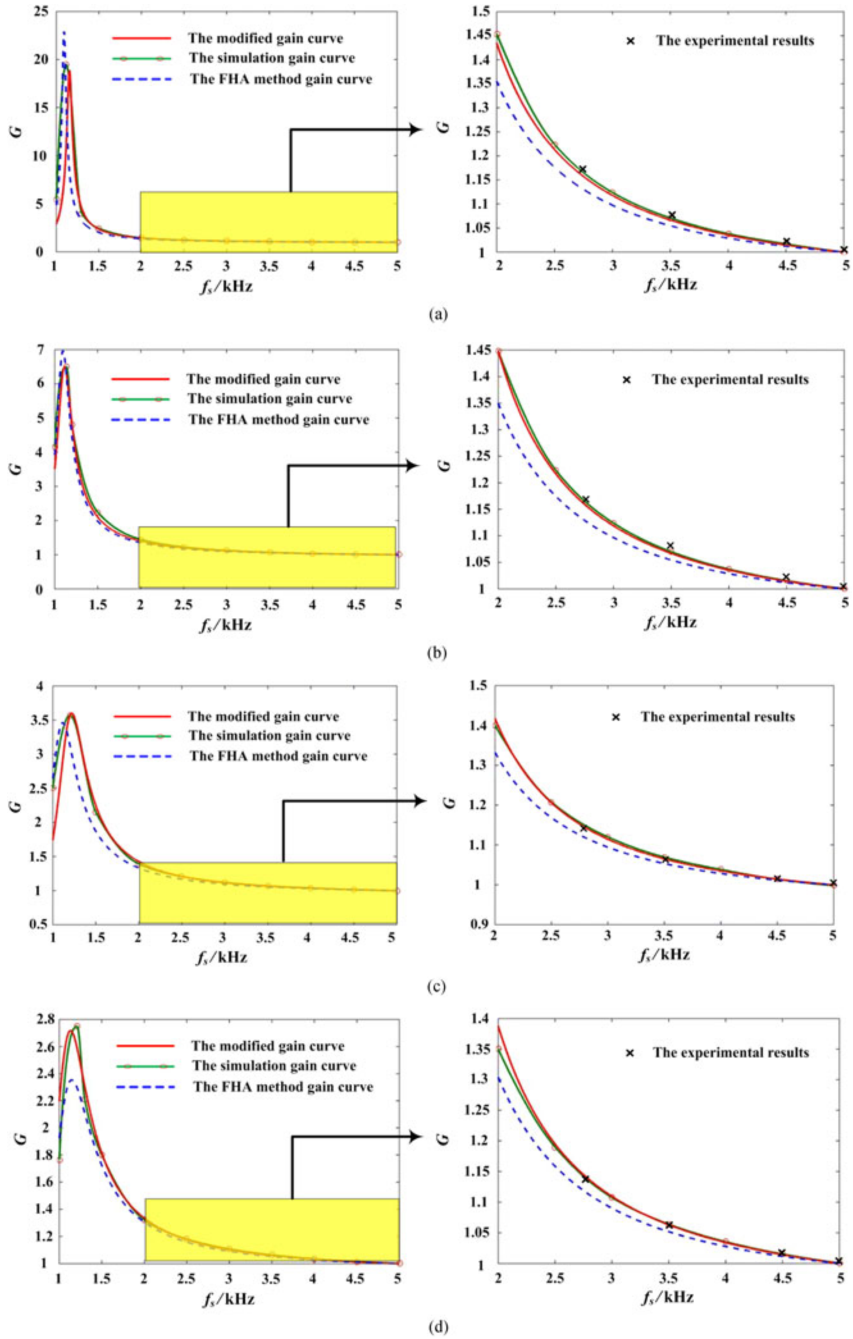

Fig. 12. Comparisons of the gain curves with different loads (the curves on the right are enlarged curves of the boxes on the left). (a) $R_L = 50\,\Omega$. (b) $R_L = 20\,\Omega$. (c) $R_L = 6.2\,\Omega$. (d) $R_L = 4.8\,\Omega$.

Substitute the above results into (33) and refer to (41), the resonant inductance L_r and resonant capacitance C_r can be finally calculated as $L_r = 111\,\mu$H and $C_r = 9\,\mu$F. And, because $k = 20$, the excitation inductance can be derived as $L_m = 2.22$ mH.

V. Simulation and Experimental Results

On the basis of the results calculated in Section IV, the final parameters of the *LLC* resonant converter are listed in Table II. According to the parameters, a simulation model-based MATLAB is built, and the simulation results of the gain curves of the *LLC* resonant converter under different load conditions are acquired. To verify the accuracy of the proposed gain model, the gain curves derived from the FHA method and the modified gain model are all given to make comparisons that are shown in Fig. 12.

From Fig. 12, on the one hand, the peak gain point derived from the modified gain model can keep up with the simulation results, and on the other hand, the gains at other frequency ranges are still accurate. Thus, the modified gain model is a universal model that can not only feed the requirement of peak gain but can also provide precise gain at full range of loads. According to the previous analysis, there are mainly two factors

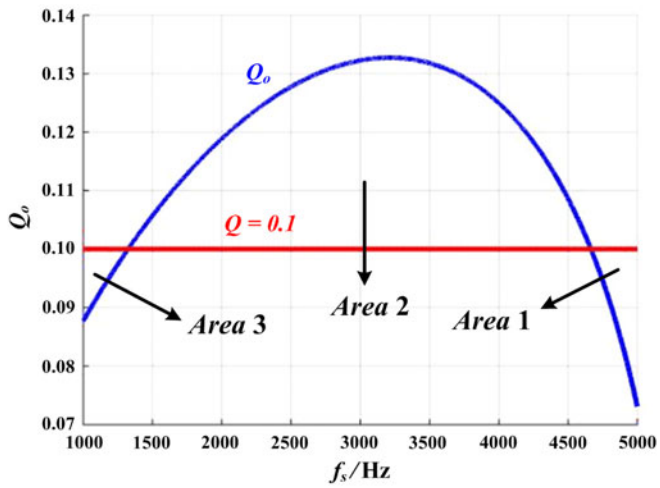

Fig. 13. Curve of Q_o with 100% load.

that can influence the accuracy of the gain model of the *LLC* resonant converter—resonant factor *A* and load factor *B*. After modification, the two factors are expressed as A_o and B_o. Then, how do the two factors influence the gain model?

It has been known from the FHA method that when quality factor *Q* (corresponding to load factor *B*) is constant, decreasing inductor ratio *k* (corresponding to resonant factor *A*) can improve the peak gain but decrease the adjustable frequency area. When inductor ratio *k* is constant, decreasing quality factor *Q* can also improve the peak gain but have little effect on the adjustable frequency area. However, for the FHA method, once *k* and *Q* are confirmed, they will not change with frequency anymore. Thus, it is hard to evaluate which factor is the leading factor of the *LLC* resonant converter. For the modified gain model, the influence of the two factors can be discussed referring to (33). Equation (33) provides a connection with Q and Q_o. We take a 100% load condition as an example, that is, the output resistance is 4.8 Ω. Substitute the known conditions, including $R_L = 4.8\,\Omega$, $L_r = 111\,\mu$H, $C_r = 9\,\mu$F, into (33). Then, the curve of Q_o can be represented in Fig. 13. In Fig. 13, $Q = 0.1$ is calculated from $Q = \frac{\sqrt{L_r/C_r}}{R_{\text{eq}}}$ based FHA method.

From Fig. 13, it can be seen the influence of quality factor is variable. In Area 1 and Area 3, it has passive effect that can increase the gain compared with the FHA method. In Area 2, it has negative effect that can decrease the gain compared with the FHA method. As expressed in Fig. 6, with the increasing of load, the errors caused by the FHA method become pretty large. The reason is that the influence of Area 3 is neglected by using the FHA method. However, as discussed before, Area 2 has negative effect on gain. Why the Area 2 does not decrease the gain in the proposed modified gain model? That because the influence of the inductor ratio *k*. Comparing $A = 1+\frac{1}{k}(1 - \frac{f_r^2}{f_s^2})$ and $A_{o1} = 1 + \frac{4\pi^2}{32k}(1 - \frac{f_r^2}{f_s^2})$, the only change is the ratio $\frac{1}{k}$ varies to $\frac{4\pi^2}{32k}$. Define modified inductor ratio $k_o = \frac{32}{4\pi^2}k \approx 0.81k$. That means the modified inductor has passive effect on increasing the gain of the *LLC* resonant converter. That is to say the influence of the modified k_o counteracts the influence of Area 2. Besides, there is still a question—as expressed before, the modified inductor ratio and quality factor all should have passive effect on the peak gain point, but why the peak gain point derived by modified gain model is lower than the peak point derived by the FHA method at light load shown in Fig. 12(a)? The reason is at light load, the influence of quality factor Q_o (corresponding to load factor B_o) is reduced and referring to (24), and the modified inductor ratio A_{o2} starts to have negative effect at peak gain point.

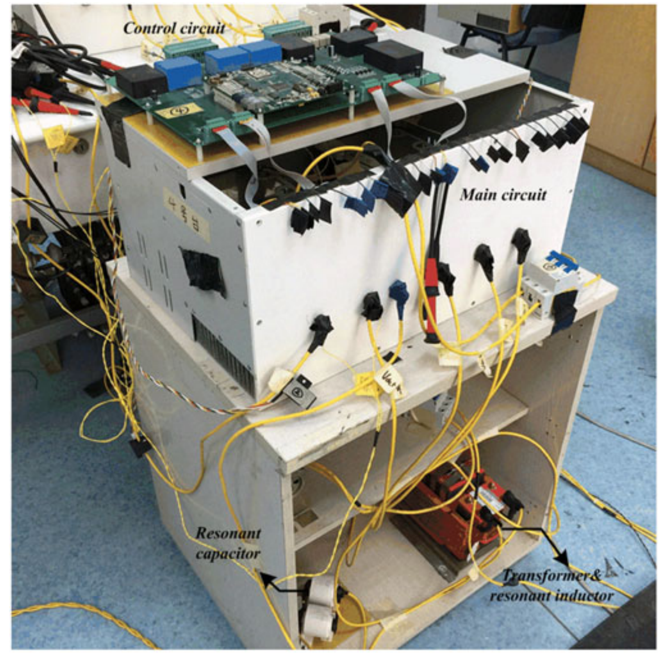

Fig. 14. Prototype of one unit of PETT.

To further verify the validity of the proposed modified gain model, a prototype of PETT is developed. One of the units is shown in Fig. 14. It is composed of a four quadrant rectifier and an *LLC* converter. For this prototype, 220 V ac is converted to 350 V dc by a four quadrant rectifier, and 350 V dc is further converted to 120 V dc by an *LLC* resonant converter. In this prototype, the rated power of each unit is 3 kW. The parameters of the *LLC* resonant converter are listed in Table II, which are the same as the calculated results in Section IV.

Fig. 15 presents the experimental waveforms of different loads (from 10% to 100% load). In each picture, the waveforms are respectively the collector-to-emitter voltage, driver pulse, resonant current and output voltage from the top down. The switching frequency of the four conditions are respectively 3450, 3373, 3354, and 3327 Hz. Put the experimental results into Table III and make comparisons with the results derived from the proposed modified gain model and the gain model based FHA method. In Table III, the error is calculated as

$$\text{error} = \frac{f_{\text{ps}} - f_{\text{ts}}}{f_{\text{ps}}} \times 100\% \qquad (42)$$

where f_{ps} is the practical switching frequency and f_{ts} is the calculated theoretical switching frequency.

It can be seen that the proposed modified gain model is pretty precise and the maximum error is only 1.2%, which is much

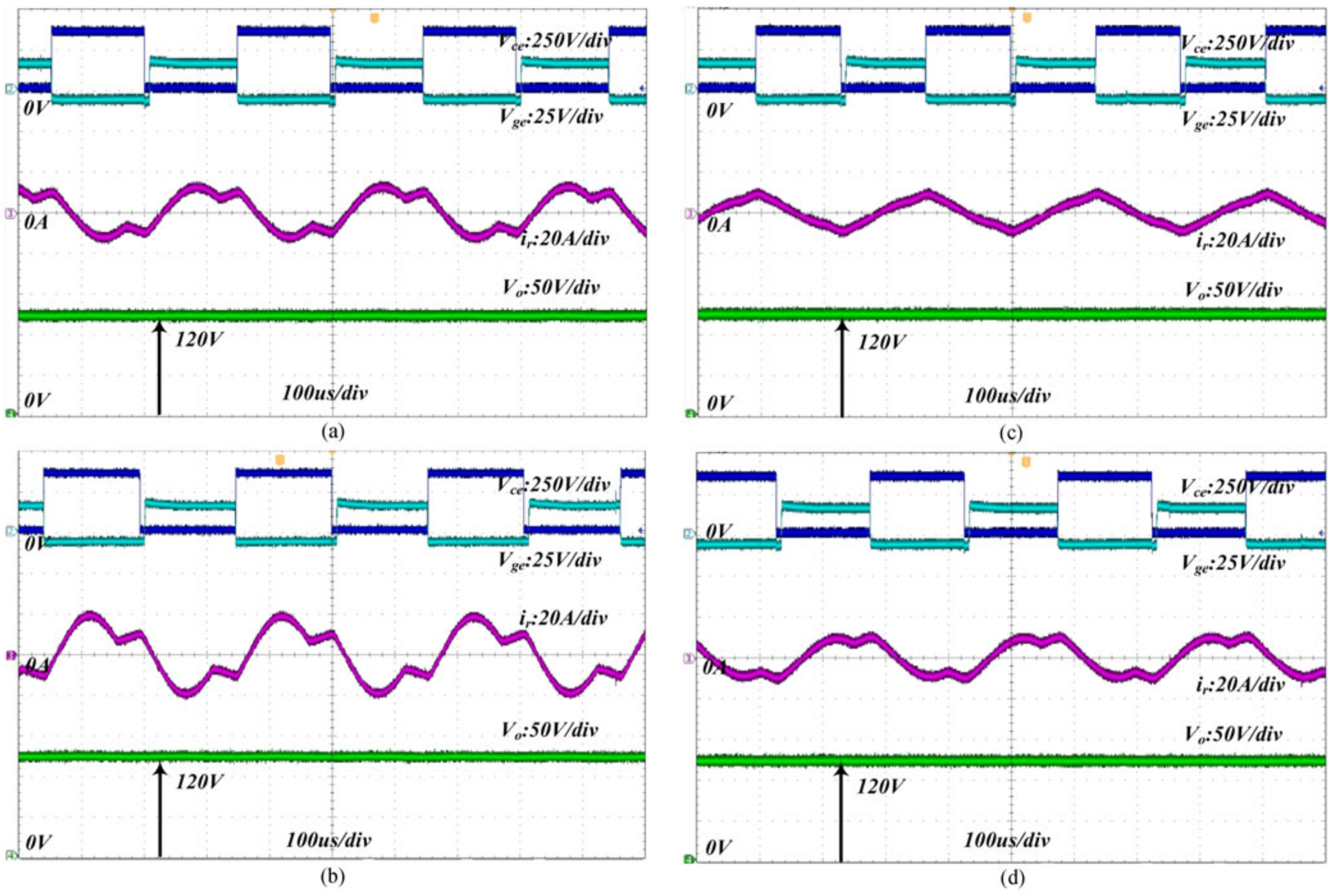

Fig. 15. Experimental curves at different loads. (a) 10% load. (b) 30% load. (c) 70% load. (d) 100% load.

TABLE III
COMPARISONS OF THE EXPERIMENTAL RESULTS AND THEORETICAL RESULTS

Gain model	The modified gain model				The gain model based FHA method			
Output power	0.3 kW	1 kW	2 kW	3 kW	0.3 kW	1 kW	2 kW	3 kW
Theoretical switching frequency	3408	3373	3354	3327	3180	3168	3147	3109
Practical switching frequency	3450	3378	3333	3305	3450	3378	3333	3305
Errors	1.2%	0.15%	0.63%	0.67%	7.8%	6.2%	5.6%	5.9%

lower than the results-based FHA method (whose maximum error is 7.8%). Refer to the simulation results in Fig. 11 and the error at peak gain point based, the modified gain model is still only 3% and the error at peak gain point based FHA method can reach up to 14%. Thus, the proposed modified gain model has good accuracy under different load conditions which can help obtain better parameters of the *LLC* resonant converter.

VI. CONCLUSION

This paper proposes a modified gain model of the *LLC* resonant converter. The modified gain model is obtained by the combinations of frequency domain analysis and time domain analysis. And two main factors which are respectively resonant factor *A* and load factor *B* are modified. The proposed gain model has following advantages:

1) The proposed gain model inherits the structure of the gain model based FHA method. Thus, there are still only two degrees of freedom (k_o and Q_o) to consider to design an *LLC* resonant converter that can not only highly simplify the design procedure but also optimize the parameters.
2) The accuracy of the modified gain model is pretty high at full range of loads which can help further discuss the characteristics of the *LLC* resonant converter, such as parameters optimization, controller design, no-load operation, short-circuit operation, and soft-start.
3) The design procedures of the *LLC* resonant converter-based proposed modified gain model are clear and independent which can be rapidly obtained by software algorithm.

REFERENCES

[1] B. Yang, F. C. Lee, A. J. Zhang, and G. Huang, "LLC resonant converter for front end DC/DC conversion," in *Proc. 17th Annu. IEEE Appl. Power Electron. Conf. Expo.*, Dallas, TX, USA, 2002, vol. 2, pp. 1108–1112.

[2] J. H. Jung, H. S. Kim, M. H. Ryu, and J. W. Baek, "Design methodology of bidirectional CLLC resonant converter for high-frequency isolation of DC distribution systems," *IEEE Trans. Power Electron.*, vol. 28, no. 4, pp. 1741–1755, Apr. 2013.

[3] B. Lu, W. Liu, Y. Liang, F. C. Lee, and J. D. Van Wyk, "Optimal design methodology for LLC resonant converter," in *Proc. 21st Annu. IEEE Appl. Power Electron. Conf. Expo.*, Dallas, TX, USA, 2006, pp. 533–538.

[4] R. Beiranvand, M. R. Zolghadri, B. Rashidian, and S. M. H. Alavi, "Optimizing the LLC–LC resonant converter topology for wide-output-voltage and wide-output-load applications," *IEEE Trans. Power Electron.*, vol. 26, no. 11, pp. 3192–3204, Nov. 2011.

[5] B. C. Hyeon and B. H. Cho, "Analysis and design of the half bridge magnetizing inductor resonant(LmC) dc/dc converter," in *Proc. 25th Annu. IEEE Appl. Power Electron. Conf. Expo.*, Palm Springs, CA, USA, 2010, pp. 1373–1377.

[6] E.-S. Kim *et al.*, "A low profile LLC resonant converter using novel planar transformer," in *Proc. Appl. Power Electron. Conf. Expo.*, 2012, pp. 1307–1312.

[7] B.-C. Kim, K.-B. Park, C.-E. Kim, B.-H. Lee, and G.-W. Moon, "LLC resonant converter with adaptive link-voltage variation for a high-powerdensity adapter," *IEEE Trans. Power Electron.*, vol. 25, no. 9, pp. 2248–2252, Sep. 2010.

[8] B. Erkmen and I. Demirel, "A very low profile dual output LLC resonant converter for LCD/LED TV applications," *IEEE Trans. Power Electron.*, vol. 29, no. 7, pp. 3514–3524, Jul. 2014.

[9] W. Feng, F. C. Lee, and P. Mattavelli, "Optimal trajectory control of LLC resonant converters for LED PWM dimming," *IEEE Trans. Power Electron.*, vol. 29, no. 2, pp. 979–987, Feb. 2014.

[10] T. Besselmann, A. Mester, and D. Dujic, "Power electronic traction transformer: efficiency improvements under light-load conditions," *IEEE Trans. Power Electron.*, vol. 29, no. 8, pp. 3971–3981, Aug. 2014.

[11] S. Moballegh, S. Madhusoodhanan, and S. Bhattacharya, "Evaluation of high voltage 15 kV for ZVS and ZCS high power DC -DC converters," in *Proc. 2014 Int. Power Electron. Conf.–ECCE Asia*, Hiroshima, Japan, 2014, pp. 656–663.

[12] D. Dujic, G. K. Steinke, M. Bellini, M. Rahimo, L. Storasta, and J. K. Steinke, "Characterization of 6.5 kV IGBTs for high-power medium-frequency soft-switched applications," *IEEE Trans. Power Electron.*, vol. 29, no. 2, pp. 906–919, Feb. 2014.

[13] C. Zhao *et al.*, "Power electronic traction transformer–Medium voltage prototype," *IEEE Trans. Ind. Electron.*, vol. 61, no. 7, pp. 3257–3268, Jul. 2014.

[14] N. Hugo, P. Stefanutti, M. Pellerin, and A. Akdag, "Power electronics traction transformer," in *Proc. 2007 Eur. Conf. Power Electron. Appl.*, Aalborg, Denmark, 2007, pp. 1–10.

[15] W. Sun, H. Wu, H. Hu, and Y. Xing, "Design considerations and experimental evaluation for LLC resonant converter with wide battery voltage range," in *Proc. 2014 IEEE Conf. Expo Transp. Electrification Asia-Pacific*, Beijing, China, 2014, pp. 1–6.

[16] J.-H. Jung and J.-G. Kwon, "Theoretical analysis and optimal design of LLC resonant converter," in *Proc. 2007 Eur. Conf. Power Electron. Appl.*, Aalborg, Denmark, 2007, pp. 1–10.

[17] S. De Simone, C. Adragna, C. Spini, and G. Gattavari, "Design-oriented steady-state analysis of LLC resonant converters based on FHA," in *Proc. Int. Symp. Power Electron. Electr. Drives Autom. Motion*, Taormina, Italy, 2006, pp. 200–207.

[18] X. Xie, J. Zhang, C. Zhao, Z. Zhao, and Z. Qian, "Analysis and optimization of LLC resonant converter with a novel over-current protection circuit," *IEEE Trans. Power Electron.*, vol. 22, no. 2, pp. 435–443, Mar. 2007.

[19] G. Ivensky, S. Bronshtein, and A. Abramovitz, "Approximate analysis of resonant LLC DC-DC converter," *IEEE Trans. Power Electron.*, vol. 26, no. 11, pp. 3274–3284, Nov. 2011.

[20] X. Fang *et al.*, "Efficiency-oriented optimal design of the LLC resonant converter based on peak gain placement," *IEEE Trans. Power Electron.*, vol. 28, no. 5, pp. 2285–2296, May 2013.

[21] X. Fang, H. Hu, Z. J. Shen, and I. Batarseh, "Operation mode analysis and peak gain approximation of the LLC resonant converter," *IEEE Trans. Power Electron.*, vol. 27, no. 4, pp. 1985–1995, Apr. 2012.

[22] C. H. Chang, E. C. Chang, C. A. Cheng, H. L. Cheng, and S. C. Lin, "Small signal modeling of LLC resonant converters based on extended describing function," in *Proc. 2012 Int. Symp. Comput. Consumer Control*, Taichung, Taiwan, pp. 365–368, 2012.

[23] R. Beiranvand, B. Rashidian, M. R. Zolghadri, and S. M. H. Alavi, "Optimizing the normalized dead-time and maximum switching frequency of a wide-adjustable-range LLC resonant converter," *IEEE Trans. Power Electron.*, vol. 26, no. 2, pp. 462–472, Feb. 2011.

[24] Z. Hu, L. Wang, H. Wang, Y. F. Liu, and P. C. Sen, "An accurate design algorithm for LLC resonant converters—Part I," *IEEE Trans. Power Electron.*, vol. 31, no. 8, pp. 5435–5447, Aug. 2016.

[25] Z. Hu, L. Wang, Y. Qiu, Y. F. Liu, and P. C. Sen, "An accurate design algorithm for LLC resonant converters—Part II," *IEEE Trans. Power Electron.*, vol. 31, no. 8, pp. 5448–5460, Aug. 2016.

Jianqiang Liu (M'13) received the B.E. and Ph.D. degrees in electrical engineering from Beijing Jiaotong University, Beijing, China, in 2003 and 2008, respectively.

He is currently an Associate Professor in the School of Electrical Engineering and a Research Scientist in the Institute of Power Electronics and Electric Traction, Beijing Jiaotong Universtity, Beijing, China. His research work is related to electric energy conversion, control of ac machines and traction drive system.

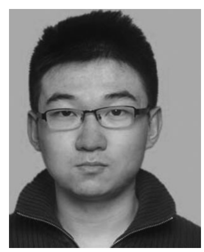

Jiepin Zhang (SM'16) was born in Xinxiang, Henan, China, in 1991. He received the B.S. degree in electrical engineering from Beijing Jiaotong University, Beijing, China, in 2014, where he is now working toward the Ph.D. degree on power electronics.

His research interests include modeling of dc–dc converters, stability of cascaded converters, and power electronics traction transformer.

Trillion Q. Zheng (M'06–SM'07) was born in Jiangshan, Zhejiang, China, in 1964. He received the B.S. degree in electrical engineering from Southwest Jiaotong University, Sichuan, China, in 1986 and the M.S. and Ph.D degrees in electrical engineering from Beijing Jiaotong University, China, in 1992 and 2002, respectively.

He is currently a University Distinguished Professor at Beijing Jiaotong University, Beijing , China. He directs the Center for Electric Traction, founded by the Ministry of Education, China. His research interests include power supply and ac dirve of railway traction systems, high performance and low loss for power electronics systems, PV-based converters and control, and active power filter and power quality correction. He holds 17 China patents, and has published more than 60 journal articles and more than 100 technical papers in conference proceedings.

From 2003 to 2011, he served as the Dean in the School of Electrical Engineering, Beijing Jiaotong University. He is currently the Deputy Director of Council of Beijing Society for Power Electronics and a Member of Council of China Electrotechnical Society.

He received the Excellent Teacher Award of Beijing Government in 1997, the Youth Award of Railway Science and Technology of Zhan Tianyou in 2005. He was Laureates of Youth Elite of Science and Technology, Railway Ministry of China in 1998 and of Zhongda Scholar for power electronics and motor drive area, by Delta Environmental and Educational Foundation in 2007.

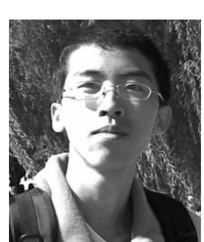

Jingxi Yang (SM'16) was born in Shangtou, Guangdong, China, in 1991. He received the B.S. degree in electrical engineering from Beijing Jiaotong University, Beijing, China, in 2014. He is currently working toward the Ph.D. degree in the School of Electrical Engineering, Beijing Jiaotong University.

His research interests include digital processing in power electronics system and power electronics transformer.